www.nature.com/leu



### LETTERS TO THE EDITOR

# Specificity and mechanism-of-action of the JAK2 tyrosine kinase inhibitors ruxolitinib and SAR302503 (TG101348)

Leukemia (2014) 28, 404-407; doi:10.1038/leu.2013.205

Activating point mutations in the JAK2 kinase were identified in BCR-ABL-negative myeloproliferative neoplasms, including polycythemia vera, essential thrombocythemia and primary myelofibrosis (MF).<sup>1,2</sup> This encouraged the development of several small-molecule JAK2 tyrosine kinase inhibitors,<sup>3</sup> of which ruxolitinib (formerly known as INCB018424) was approved by the US Food and Drug Administration for the treatment of patients with intermediate or high-risk MF, including primary MF, postpolycythemia vera MF and post-essential thrombocythemia MF.<sup>4,5</sup> Another JAK2 inhibitor, SAR302503 (formerly known as TG101348), is in advanced clinical trials.<sup>6,7</sup> Both drugs inhibit JAK2 kinase activity in vitro and JAK2-dependent proliferation of cell lines with IC<sub>50</sub> values in the low nanomolar concentration range.<sup>8,9</sup> Among the four kinases of the JAK family (JAK1, JAK2, JAK3 and TYK2), SAR302503 also inhibits JAK1, Tyk2 and JAK3, albeit with  $\sim$  30-,  $\sim$  100- and  $\sim$  300-fold weaker efficiency than JAK2, respectively.9 Ruxolitinib inhibits JAK1 and JAK2 equally well, and targets TYK2 > 10-fold and JAK3 ~ 100-fold weaker.8 As both drugs were only tested for inhibition of a few dozen unrelated kinases, 9,8 accounting for only a small portion of the 518 human kinases, comprehensive data on their specificity are missing. In addition, no structural data of ruxolitinib or SAR302503 bound to the JAK2 kinase domain that would reveal their binding modes and molecular mechanism-of-action are available. Of note, ruxolitinib is the only FDA-approved kinase inhibitor for which no co-crystal structure with its target kinase has been published. 10 Here, we present a near-kinome-wide survey of the specificity of ruxolitinib and SAR302503 and determine their binding modes to the JAK2 kinase domain by extensive sampling using molecular dynamics (MD) simulations.

For specificity testing, we used a panel consisting of 368 recombinant human kinases (including 70 kinase mutants relevant to human disease), thereby covering  $\sim 60\%$  of the human kinome. Inhibition of the kinase activity in vitro was assayed for both drugs in parallel at a concentration of 1.0 μм. Ruxolitinib inhibited the activity of 33 kinases (including 11 kinase mutants) by ≥50%, whereas 54 kinases (including 14 kinase mutants) were inhibited by SAR302503 (Table 1a and Supplementary Data). Eleven and 14 kinases (including 2 and 4 kinase mutants, respectively) were inhibited by ruxolitinib and SAR302503, respectively, by ≥80% (Table 1a). We subsequently determined the IC50 values for kinases that showed profound inhibition in the tested panel. We concentrated on known oncogenes and/or validated drug targets in cancer and other diseases. These included the receptor tyrosine kinases ALK, RET, TRK-B, the cytoplasmic tyrosine kinases ACK1, FAK, LCK and the serine/threonine kinase JNK1. Ruxolitinib strongly inhibited TRK-B ( $IC_{50} = 11 \text{ nm}$ ), as well as ACK1, ALK and RET with  $IC_{50}$  values below 300 nm. SAR302503 inhibited LCK and RET with IC50 values  $\sim$  500 nm, and ACK1, FAK and JNK1 with IC<sub>50</sub> values  $\sim$  200 nm (Table 1b) in addition to the previously described inhibition of FLT3 and BCR-ABL.9,11 We were intrigued when we found LRRK2 and

several of its pathogenic mutants, which are common causes of familial Parkinson's disease, 12 to be profoundly inhibited by both JAK2 inhibitors (Table 1a). We then used in vitro kinase inhibition assays for LRRK2 and monitored the cellular phosphorylation of LRRK2 at Ser-910/935 as a pharmacodynamic marker of LRRK2 kinase activity. LRRK2 kinase activity was inhibited in vitro with IC50 values 820 nm and 1.8 um for ruxolitinib and SAR302503, respectively (Table 1b), but both drugs were not able to strongly inhibit the LRRK2 phosphorylation at Ser-910/935 in cells (data not shown). SAR302503 inhibits a much larger number of off-target tyrosine kinases than ruxolitinib (31 vs 15, excluding the JAK kinases), whereas the number of off-target serine-/threonine kinases is similar for both drugs. The tyrosine kinases that are targeted by SAR302503, but not by ruxolitinib, include the SRC family kinases LCK and FGR, the T-cell kinase ITK, as well as the KIT and FLT3 receptor kinases, all of which are critical for hematopoietic cell signaling. In addition, SAR302503 targets kinases that are predominantly expressed in non-hematopoietic cells, such as PDGFR members and DDR2. Those are thought to contribute to the side-effect profile of BCR-ABL tyrosine kinase inhibitors. Based on these observations, one may speculate on a higher incidence of adverse events in patients treated with SAR302503, as compared with ruxolitinib.

The detailed knowledge of the binding mode of a kinase inhibitor at the atomic level is essential to understand its mechanism-of-action, interpret its specificity, predict and rationalize its resistance mechanisms, and suggest points of chemical derivatization for improved potency and specificity. To shed light on the binding mode of ruxolitinib and SAR302503 to JAK2, we carried out multiple runs of MD simulations (simulation protocols and analyses of MD trajectories are in the Supplementary Information). MD is a computational method to assess the structure and flexibility of proteins and their interactions with ligands. Notably, we performed simulations with explicit solvent and full flexibility of both JAK2 and inhibitor, that is, taking into account not only enthalpic but also entropic contributions of drug binding. It is important to note that MD simulations are significantly more accurate (albeit computationally more expensive) than the commonly used docking with rigid protein targets. Following a similar MD-based simulation protocol, we previously predicted the binding mode of a potent ATP-competitive inhibitor of the EphB4 tyrosine kinase, which is essentially identical to the subsequently determined crystal structure.<sup>13</sup> The MD simulations (cumulative sampling of 1.5 and 0.1 µs for ruxolitinib and SAR302503, respectively) suggest that both drugs inhibit JAK2 by a so-called type I binding, in which the inhibitor targets the ATPbinding site of the kinase in its active conformation and the DFGmotif at the base of the activation loop is in its inward-facing conformation. 14 Importantly, the analysis of the free-energy surface (Supplementary Figures S2 and S3) and displacement from the starting poses indicate that there are multiple orientations for the functional groups partially exposed to solvent (Figure 1 and Supplementary Figure S4). The double-ring system (7H-pyrrolo[2,3-d]pyrimidin) of ruxolitinib is involved in two persistent hydrogen bonds with the so-called hinge region, which is the sequence segment that connects the N-lobe to the C-lobe of the kinase domain (Figures 1a and b). These two key interactions are

Table 1. Target profile of ruxolitinib and SAR302503 а Ruxolitinib SAR302503 % Inhibition % Inhibition Kinase Kinase at 1 μм at 1μM TYK2 100 IAK2 JAK2 99 TSF1 96 JAK1 97 DAPK3 96 JAK3 FGF-R1 V561M 94 96 TRK-B ACV-R1 94 90 ITK 90 MUSK 88 TRK-C 88 ACK1 87 CAMK2A 86 FAK 86 LRRK2 G2019S 84 ACV-RI 1 86 RET V804M 83 RET V804L 84 CAMK2D 80 DAPK1 84 RET V804L 78 TYK2 83 MEKK3 76 FLT3 ITD 83 ACK1 RFT V804M 82 72 ROCK1 DAPK2 79 71 AI K 69 FLT3 D835Y 78 **RET R813O** 67 PDGFR-beta 72 MEKK2 RET R813Q 72 66 DAPK3 66 JAK1 72 ROCK2 65 JNK3 69 LRRK2 wt 64 SAK 69 LRRK2 R1441C JNK2 68 62 RET wt 67 RET wt 61 LRRK2 12020T RET M918T 60 67 RET R749T 57 RET Y791F 67 DAPK1 57 **RET E762Q** 66 RFT M918T 65 57 NEK9 **RET E762Q** 57 PDGFR-alpha 65 57 65 RET Y791F **LCK** RET G691S RET G691S 55 64 CSF1-R 55 RET R749T 64 PRKG2 55 TXK 63 DAPK2 51 FGF-R1 wt 62 DDR2 61 60 RET S891A 60 LRRK2 G2019S 59 KIT V560G 59 ITK 59 59 JAK3 JNK1 58 TAOK2 57 FGF-R2 57 TGFB-R2 55 54 TRK-A AXL 54

| <i>U</i>    |                     |                      |  |
|-------------|---------------------|----------------------|--|
| Kinase      | IC <sub>50</sub> /1 | IC <sub>50</sub> /nM |  |
|             | Ruxolitinib         | SAR302503            |  |
| ACK1<br>ALK | 230<br>290          | 170<br>3400          |  |

SNF1LK2

TRK-C

Aurora-B

PRKG2

TRK-B

FGR STK33

ARK5

54

53

53

52

52

52

51

50

| Table 1. (Continued) |                  |                      |  |
|----------------------|------------------|----------------------|--|
| b                    |                  |                      |  |
| Kinase               | IC <sub>50</sub> | IC <sub>50</sub> /nM |  |
|                      | Ruxolitinib      | SAR302503            |  |
| FAK                  | 3500             | 160                  |  |
| JNK1                 | > 10000          | 260                  |  |
| LCK                  | 3600             | 500                  |  |
| RET                  | 280              | 560                  |  |
| TRK-B                | 11               | 1200                 |  |
| LRRK2 wt             | 820              | 1800                 |  |

(a) Both drugs were assayed at a concentration of 1 µM against a panel of 368 recombinant human kinases in vitro in duplicates (ProQinase assay panel). All kinases that are inhibited by more than 50% are shown in the table. (b) IC50 for inhibition of selected kinases were determined by 10 serial dilutions of the drugs in semi-log steps and calculated using Graphpad Prism. The raw data-set is presented as Supplementary Data.

preserved during all simulations of ruxolitinib (Supplementary Figure S1). In contrast, the cyclopentane ring and propanenitrile, as well as the pyrazole ring, can vary their orientations with respect to the rigid double-ring system (Figure 1a and Supplementary Figures S2–S4).

As mentioned above, the binding modes of both drugs were obtained by taking into account full flexibility of both JAK2 and the drug, as well as solvent effects. Moreover, multiple long simulations were carried out to obtain statistically significant sampling. Therefore, our MD simulations offer a first reliable structural view on the possible binding modes of ruxolitinib and SAR302503 to JAK2. It is also not surprising that the binding mode of ruxolitinib proposed here differs strongly from the one reported recently by others, which was obtained by a much simpler computational protocol, that is, rigid protein docking, and is not stable according to MD simulations (Supplementary Figure S4).

Mutation of the so-called gatekeeper residue in various kinases, such as the T315I mutation in BCR-ABL, is a common cause of resistance to kinase inhibitors in the clinical use. 10 Based on the results of our MD simulations, the hydrophobic pocket guarded by the gatekeeper residue (Met-929) is not involved in ruxolitinib and SAR302503 binding to the JAK2 kinase domain (Figure 1c). In addition, the gatekeeper residue in the identified off-target kinases of ruxolitinib and SAR302503 (Table 1) differs in size and hydrophobicity (mainly Met, Val, Thr, Phe or Leu). Together, this indicates that ruxolitinib and SAR302503 bindings are not influenced by the identity of the gatekeeper residue. This finding is in contrast to the kinases that are targeted by the BCR-ABL inhibitors imatinib, nilotinib and dasatinib, which almost exclusively contain threonine as a gatekeeper residue.<sup>16</sup> In line with these observations, a recent unbiased screen for ruxolitinib resistance mutations in a cell line model did not identify mutations of the JAK2 gatekeeper (Met-929). <sup>15</sup> In vitro inhibition assays with the JAK2 M929I gatekeeper mutant also showed only a mild increase in  $IC_{50}$  for ruxolitinib and no resistance to SAR302503, in contrast to the strong kinase inhibitor resistance conferred by gatekeeper mutations in several other kinases. 10 These results indicate that mutations in the gatekeeper residue are not expected to occur in patients treated with ruxolitinib or SAR302503. In contrast, mutations Y931C and G935R found in *in vitro* screens conferred strong resistance to ruxolitinib.<sup>15</sup> Based on the proposed binding mode (Figure 1c), the aromatic side chain of Y931 enhances the binding of the double-ring system in ruxolitinib by shielding the key hydrogen bonds with



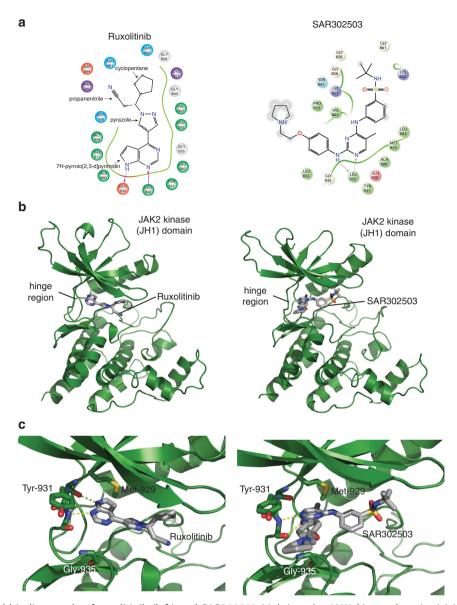


**Figure 1.** The predicted binding mode of ruxolitinib (left) and SAR302503 (right) to the JAK2 kinase domain. (a) Most populated binding mode of ruxolitinib (left) and SAR302503 (right) in the MD simulations. These two-dimensional plots were prepared with Ligplot.<sup>17</sup> They show the JAK2 residues in van der Waals contact with the drugs (green, cyan, blue, red and white circles for hydrophobic, polar, basic, acidic and glycine residues, respectively), the intermolecular hydrogen bonds (magenta arrows) and the atoms of the drugs exposed to solvent (gray circles). Ring systems and functional groups of ruxolitinib that are mentioned in the text are labeled. (b) Cartoon representation of the JAK2 kinase domain bound to ruxolitinib (left) and SAR302503 (right). As in panel (a), the most populated binding mode of the drugs in the MD simulations is shown. (c) Detailed view of the drug-binding sites. Critical hydrogen bonds to the hinge region are indicated by a yellow dotted line. Met-929 (gatekeeper residue) as well as Tyr-931 and Gly-935 that were shown to render JAK2 resistant to ruxolitinib and SAR302503 upon mutation, are shown as sticks. A detailed description of the employed methods and results can be found in Supplementary Data.

the hinge region (E930 and L932) from aqueous surroundings, which are disrupted upon Y931C mutation. The G935R mutation introduces a bulky side chain that may sterically hinder the binding of ruxolitinib. Importantly, these two mutants are also cross-resistant to SAR302503,<sup>15</sup> in line with the role of Y931 in stabilizing the binding and the steric conflicts of a bulky side chain at position 935 (Figure 1c).

In summary, we present a comprehensive survey of the near-kinome-wide specificity of ruxolitinib and SAR302503, which reveals potentially clinically relevant off-targets. Furthermore, our MD simulations suggest possible binding modes of both inhibitors. The binding modes explain the mechanism-of-action of resistance-causing point mutations that were observed *in vitro* 

and serves as a template to interpret mutations that may arise in patients treated with JAK2 inhibitors.

### **CONFLICT OF INTEREST**

The authors declare no conflict of interest.

#### **ACKNOWLEDGEMENTS**

This work was supported by the ISREC Foundation (grant to OH and SG), the Swiss National Science Foundation (grant to AC) and the Olga Mayenfisch Foundation. The MD simulations were carried out on the Schroedinger computer cluster of the University of Zurich.



T Zhou<sup>1</sup>, S Georgeon<sup>2</sup>, R Moser<sup>3</sup>, DJ Moore<sup>3</sup>, A Caflisch<sup>1,4</sup> and O Hantschel<sup>2,4</sup>

<sup>1</sup>Department of Biochemistry, University of Zürich, Zürich, Switzerland;

<sup>2</sup>Swiss Institute for Experimental Cancer Research, School of Life Sciences, École polytechnique fédérale de Lausanne, Lausanne, Switzerland and

<sup>3</sup>Brain Mind Institute, School of Life Sciences, École polytechnique fédérale de Lausanne, Lausanne, Switzerland E-mail: caflisch@bioc.uzh.ch or oliver.hantschel@epfl.ch <sup>4</sup>Joint senior authors in this study.

#### **REFERENCES**

- 1 Skoda R. The genetic basis of myeloproliferative disorders. Hematology AmSoc Hematol Educ Program 2007: 1-10.
- 2 Tefferi A, Vainchenker W. Myeloproliferative neoplasms: molecular pathophysiology, essential clinical understanding, and treatment strategies. J Clin Oncol 2011; **29**: 573-582.
- 3 Pardanani A, Vannucchi AM, Passamonti F, Cervantes F, Barbui T, Tefferi A. JAK inhibitor therapy for myelofibrosis: critical assessment of value and limitations. Leukemia 2011; 25: 218-225.
- 4 Harrison C, Kiladjian JJ, Al-Ali HK, Gisslinger H, Waltzman R, Stalbovskaya V et al. JAK inhibition with ruxolitinib versus best available therapy for myelofibrosis. N Engl J Med 2012; 366: 787-798.
- 5 Verstovsek S, Mesa RA, Gotlib J, Levy RS, Gupta V, DiPersio JF et al. A double-blind, placebo-controlled trial of ruxolitinib for myelofibrosis. N Engl J Med 2012; 366:
- 6 Pardanani A, Gotlib JR, Jamieson C, Cortes JE, Talpaz M, Stone RM et al. Safety and efficacy of TG101348, a selective JAK2 inhibitor, in myelofibrosis. J Clin Oncol 2011: 29: 789-796.

- 7 Geyer HL, Tibes R, Mesa RA. JAK2 inhibitors and their impact in myeloproliferative neoplasms. Hematology 2012; 17(Suppl 1): S129-S132.
- 8 Quintás-Cardama A, Vaddi K, Liu P, Manshouri T, Li J, Scherle PA et al. Preclinical characterization of the selective JAK1/2 inhibitor INCB018424: therapeutic implications for the treatment of myeloproliferative neoplasms. *Blood* 2010: **115**:
- 9 Wernig G, Kharas MG, Okabe R, Moore SA, Leeman DS, Cullen DE et al. Efficacy of TG101348, a selective JAK2 inhibitor, in treatment of a murine model of JAK2V617F-induced polycythemia vera. Cancer Cell 2008; 13:
- 10 Lamontanara AJ, Gencer EB, Kuzyk O, Hantschel O. Mechanisms of resistance to BCR-ABL and other kinase inhibitors. Biochim Biophys Acta 2013; 1834(7): 1449-1459.
- 11 Hantschel O, Warsch W, Eckelhart E, Kaupe I, Grebien F, Wagner K-U et al. BCR-ABL uncouples canonical JAK2-STAT5 signaling in chronic myeloid leukemia. Nat Chem Biol 2012: 8: 285-293.
- 12 Rudenko IN, Chia R, Cookson MR. Is inhibition of kinase activity the only therapeutic strategy for LRRK2-associated Parkinson's disease? BMC Med 2012; 10: 20.
- 13 Lafleur K, Dong J, Huang D, Caflisch A, Nevado C. Optimization of inhibitors of the tyrosine kinase EphB4. 2. Cellular potency improvement and binding mode validation by X-ray crystallography. J Med Chem 2013; 56: 84-96.
- 14 Liu Y, Gray NS. Rational design of inhibitors that bind to inactive kinase conformations, Nat Chem Biol 2006: 2: 358-364.
- 15 Deshpande A, Reddy MM, Schade GOM, Ray A, Chowdary TK, Griffin JD et al. Kinase domain mutations confer resistance to novel inhibitors targeting JAK2V617F in myeloproliferative neoplasms. Leukemia 2012; 26:
- 16 Hantschel O, Rix U, Schmidt U, Burckstummer T, Kneidinger M, Schutze G et al. The Btk tyrosine kinase is a major target of the Bcr-Abl inhibitor dasatinib. Proc Natl Acad Sci USA 2007: 104: 13283-13288.
- 17 Wallace AC, Laskowski RA, Thornton JM. LIGPLOT: a program to generate schematic diagrams of protein-ligand interactions. Protein Eng 1995; 8: 127-134.

Supplementary Information accompanies this paper on the Leukemia website (http://www.nature.com/leu)

## **OPEN**

# Combinatorial drug screening identifies synergistic co-targeting of Bruton's tyrosine kinase and the proteasome in mantle cell lymphoma

Leukemia (2014) 28, 407-410; doi:10.1038/leu.2013.249

We have performed a focused combinatorial screen of targeted drugs combined with ibrutinib in mantle cell lymphoma (MCL) cells, and identified the proteasome inhibitor carfilzomib as a targeted agent that could be used with ibrutinib to provide improved clinical responses. Other targeted agents that displayed cytotoxic benefit in our screen also were independent of the B-cell receptor (BCR) pathway, whereas agents within the BCR pathway did not provide benefit.

MCL is an incurable B-cell malignancy with poor prognosis. 1,2 As with many other malignancies and lymphoproliferative disorders of B-cell lineage, growth and survival of MCL depends on signaling via the BCR.<sup>3,4</sup> Potential therapeutic targets of the BCR pathway for MCL include downstream kinases LYN, SYK, PI3K and Bruton's tyrosine kinase (BTK). Ibrutinib (PCI-32765) is an orally bioavailable BTK inhibitor, which has clinical efficacy against numerous B-cell malignancies. In phase I/II clinical trials, ibrutinib elicited an overall response rate of 68% in patients with relapsed/refractory MCL, including patients previously exposed to bortezomib<sup>3</sup> and 83% in patients with relapsed/refractory chronic lymphocytic leukemia (CLL).<sup>4</sup> This is the highest response rate demonstrated by any single agent in MCL and CLL.

However, in spite of these encouraging results, responses are generally incomplete, de novo resistance is common and recurrence is anticipated, as is the case with most single-agent targeted therapies.<sup>5</sup> Treatment with a single-agent targeted drug rapidly activates a variety of redundant and compensatory signaling pathways that blunt cytotoxicity and rapidly lead to adaptive resistance.<sup>5,6</sup> Consequently, disease progression or recurrence can occur within months and is often more clinically aggressive and resistant to treatment than at initial presentation. Although the mechanisms of primary and acquired resistance to ibrutinib have yet to be elucidated, anecdotal reports suggest that MCL disease progression on ibrutinib can be aggressive and often refractory to other treatments, indicating that compensatory signaling changes and adaptive resistance have occurred. In addition, acquisition of mutations of BTK that impact ibrutinib binding was recently observed in CLL cells. We hypothesize that drug combinations that block adaptive signaling responses can

Accepted article preview online 27 August 2013; advance online publication, 8 October 2013